Effect of intertube interaction on the transport properties of a carbon double-nanotube device

Xiao-Fei Li, Ke-Qiu Chen, Ling-Ling Wang, Meng-Qiu Long, B. S. Zou, and Z. Shuai

Citation: Journal of Applied Physics **101**, 064514 (2007); doi: 10.1063/1.2714780
View online: https://doi.org/10.1063/1.2714780
View Table of Contents: http://aip.scitation.org/toc/jap/101/6
Published by the American Institute of Physics

Effect of intertube interaction on the transport properties of a carbon double-nanotube device

Xiao-Fei Li, Ke-Qiu Chen,[a] Ling-Ling Wang,[b] Meng-Qiu Long, and B. S. Zou
Department of Applied Physics, Hunan University, Changsha 410082, China

Z. Shuai
Key Laboratory of Organic Solids, Institute of Chemistry, Chinese Academy of Sciences, Beijing 100080, China

(Received 7 December 2006; accepted 24 January 2007; published online 28 March 2007)

By applying nonequilibrium Green's functions and first-principles calculations, we investigate the transport behaviors of the bitube device with two single-walled nanotubes attached to metal electrodes. The results show that the intertube interactions play an important role in the conducting behavior of these systems. By adjusting the intertube distance and the orientational order, namely changing the magnitude of the intertube interactions, a different transport behavior can be observed in the system. © *2007 American Institute of Physics*. [DOI: 10.1063/1.2714780]

I. INTRODUCTION

In the past decade, the electronic transport properties of single-molecule junctions or molecular devices have attracted much attention. Various kinds of single-molecule junctions or molecular monolayer junctions, such as short organic molecule wires,[1–11] long-chain polymers,[12,13] fullerenes,[14,15] carbon nanotubes,[16] and so on, have been reported. In particular, molecular junctions constructed by carbon nanotubes are the systems intensely studied because of their unique one-dimensional geometry, mechanical and chemical robustness, and excellent transport property. Several metal-nanotube-metal junctions have been studied experimentally.[17–19] Theoretically, the electronic transport properties of single-walled nanotube (SWNT) junctions have also been studied extensively. Pomorski *et al.*[20] calculated the current voltage (*I-V*) characteristics of prototypical short semiconducting nanotubes coupled to metallic leads by using nonequilibrium Green's function formalism combined with density functional theory based simulations. They found the metallic behavior in the system and suggested that this behavior is due to the presence of evanescent modes. Xue and Ratner[21] presented an analysis of the electronic transport properties of the metal-SWNT-metal junction with the length of SWNT being varied from the nanometer to tens of nanometer range. Their results showed a transition from tunneling to thermal activation-dominated transport with increasing nanotube length. Wu *et al.*[22] predicted a pressure-induced metal to semiconductor transition in armchair SWNTs. The transport properties of multiwalled carbon nanotubes (MWNTs) have also been reported theoretically[23] and experimentally[24,25] and showed that the inner shells can contribute to the total conductance and the inner-shell hopping can play a crucial role in MWNTs transport. However, there are very few reports on the effect of intertube coupling on the transport properties of the molecular junction with two or more single-walled carbon nanotubes sandwiched between metal electrodes. In spite of there being a number of reports on intertube coupling effects on electronic structures in systems including two or more nanotubes such as carbon nanotube bundles or ropes,[26–29] most of the theoretical analyses to date are based on infinite carbon nanotubes, whose characteristics are fundamentally different from those of the finite tubes coupled to metal electrodes.

In the present work, we consider such a system: two semiconducting (8, 0) SWNTs coupled to Al leads, as given in Fig. 1. Our work focuses primarily on the effect of intertube interaction on the transport properties of the molecular junction. The calculated results show that the intertube interaction can induce a different conducing behavior in the system.

II. MODEL AND COMPUTATIONAL METHOD

Figure 1 shows a schematic of molecular device with part of the electrodes. Typically, in the contact region, a supercell is consisted of a 5×9 (100) two layers of Al slab with 45 atoms per unit cell in the left lead, and a three layers of Al slab with 67 atoms in the right lead, and 256 (4 cells for each tubes) carbon atoms for two semiconducting (8, 0) nanotubes in the central scattering region. To evaluate the effect of the metal-SWNT interface coupling, we consider

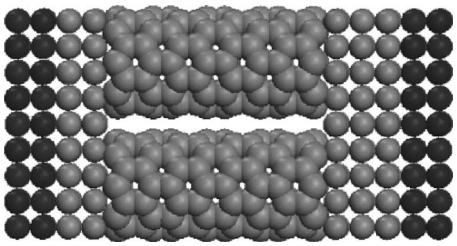

FIG. 1. Two-probe device configuration with two (8, 0) carbon nanotubes between two Al electrodes. A supercell consisted of a 5×9 (100) two layers of Al slab with 45 atoms per unit cell in the left lead, and three layers of Al slab with 67 atoms in the right lead, and 256 (four cells for each tubes) carbon atoms for two semiconducting (8, 0) nanotubes is the device scattering region.

[a]Electronic mail: keqiuchen@hnu.cn
[b]Electronic mail: llwang@hnu.cn

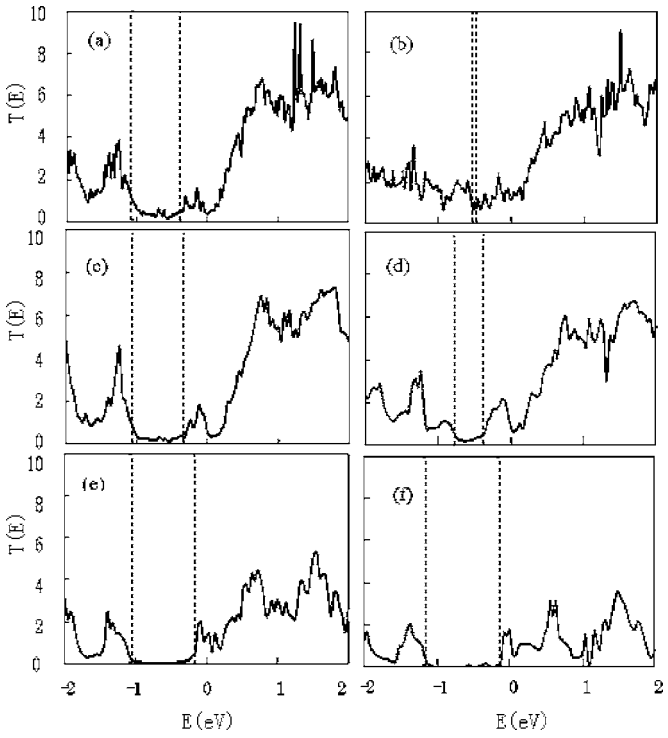

FIG. 2. The transmission spectra $T(E, V_b)$ as a function of electron energy at zero bias (V_b=0): (a)–(e) is for the bitubes system shown in Fig. 1, and (f) for the the single (8, 0) SWNT junction with the same parameters as Fig. 2(e). Figures 2(a) and 2(b) correspond to intertube distances L_{t-t}=3.0 Å and L_{t-t}=2.3 Å with electrode-tube distance L_{e-t}=1.8 Å and the rotational angle φ=0 (namely hexagon-to-hexagon ordering between the two tubes), respectively; (c) and (d) correspond to the rotational angle $\varphi=2\pi/16$ [namely the maximum rotational angle by rotating one tube around the long tube-axis as a result of the D_{8h} symmetry of the (8, 0) tube] with the same electrode-tube distance and intertube distances as (a) and (b), respectively; (e) is of the same intertube distance and rotational angle as (a) but with electrode-tube distance L_{e-t}=2.3 Å. The vertical dashed lines represent the positions of the molecular orbital HOMO (left) and LUMO (right), respectively. The energy origin is set to be the Fermi level of the system.

the SWNT end-metal surface distance varying from 1.8 to 2.3 Å, which is the typical range of electrode-tube distance employed in most of the references.[20,21] Note that the finite SWNT molecules are attached to the electrode surface through the ring of dangling-bond carbon atoms at the ends. Here, we neglect the possible distortion of the SWNT atomic structure induced by the open end. The method for the quantum transport calculation we use here is a first-principle nonequilibrium Green's function-based electronic transport package, TranSIESTA-C.[30,31] This method is based on density functional theory and can treat the molecule-electrode system self-consistently under finite bias conditions.

III. RESULTS AND DISCUSSION

In Figs. 2(a)–2(e), we present the transmission spectra $T(E, V_b)$ as a function of electron energy at zero bias (V_b =0) for the bitube system shown in Fig. 1: Figs. 2(a) and 2(b) correspond to intertube distances L_{t-t}=3.0 Å and L_{t-t} =2.3 Å with electrode-tube distance L_{e-t}=1.8 Å and the rotational angle φ=0 (namely hexagon-to-hexagon ordering between the two tubes), respectively; Figs. 2(c) and 2(d) correspond to the rotational angle $\varphi=2\pi/16$ [namely the maximum rotational angle by rotating one tube around the long tube-axis as a result of the D_{8h} symmetry of the (8, 0) tube] with the same electrode-tube distance and intertube distance as Figs. 2(a) and 2(b), respectively; Fig. 2(e) is of the same intertube distance and rotational angle as Fig. 2(a) but with electrode-tube distance L_{e-t}=2.3 Å. As a comparison, in Fig. 2(f), we give the transmission coefficient of the single (8, 0) SWNT junction with the same parameters as Fig. 2(e). It is known that the transmission spectra reflects the electronic structure of the molecule and the coupling, which mediates the electronic transport.[20,21,32] From Fig. 2(a), it is seen clearly a wide valley with small transmission about the Fermi level. When the intertube distance L_{t-t} is decreased, the transmission coefficient increases and the transmission valley is gradually broken, as found from Fig. 2(b). By comparing Figs. 2(c) and 2(d) with Figs. 2(a) and 2(b), we find that the transmission is more favorable for the configuration that the two tubes are placed in hexagon-to-hexagon order (namely the rotational angle being zero). According to the D_{8h} symmetry of the (8, 0) tube, the range of the rotational angle is spanned between 0 and $2\pi/16$. The calculation shows that the transmission coefficient becomes smaller with increasing the rotational angle. From Fig. 2(e), we can see that with an increase in the electrode-tube distance, the extent of primary tunneling from the molecule to the electrode is reduced drastically, and a fully gap is developed about the Fermi level, which shows semiconducting behavior of the system. This results from the fact that the coupling between the electrodes and the tubes becomes weaker when the electrode-tube distance is increased. When comparing Fig. 2(f) with Figs. 2(a)–2(e), we find that more transmission peaks appear in the bitubes systems, which mean that more transmission channels are open in this system than in the single-molecule system. Moreover, peak values and their positions of the single-molecule system are different from those of the bitubes system. These results indicate that the intertube interaction play an important role in electronic transport for the bitubes system.

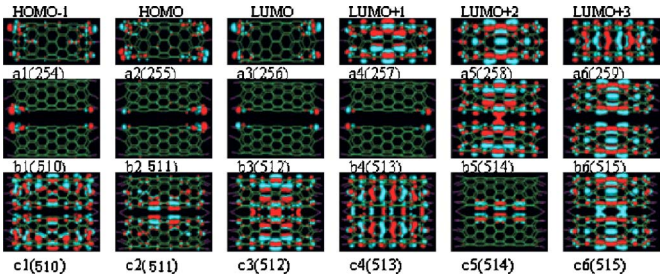

FIG. 3. (Color online) Frontier orbitals of the MPSH. (a1)–(a6) show six frontier molecular orbits of the MPSH for the monotube system: Orbits 254–259 correspond to HOMO−1, HOMO, LUMO, LUMO+1, LUMO +2, and LUMO+3, respectively; (b1)–(b6) and (c1)–(c6) show six frontier molecular orbits from HOMO−1 to LUMO+3 for the bitubes system with intertube distance L_{t-t}=3.0 Å and L_{t-t}=2.3 Å, respectively.

To further understand the nature of the intertube interaction, in Fig. 3, we give the molecularly projected self-consistent Hamiltonian (MPSH), which is the molecular part extracted from the whole self-consistent Hamiltonian for the contact region (two layers of Al electrode in the left with the bitubes and three Al layers on the right side). Note that

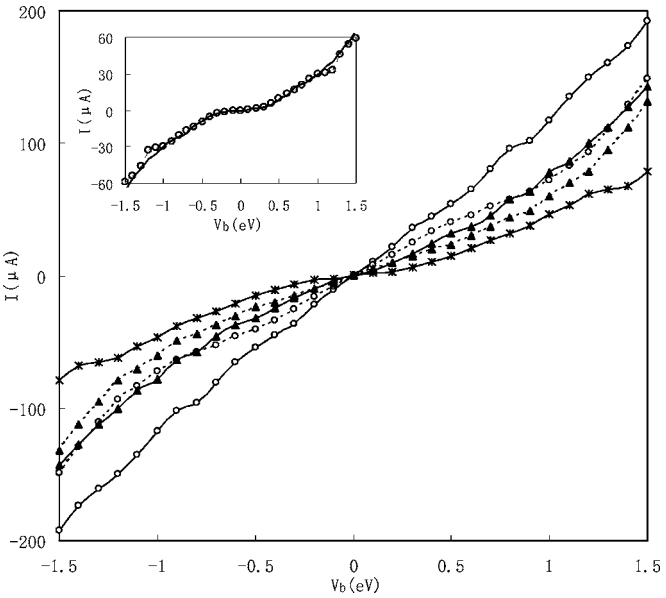

FIG. 4. *I-V* curves of the bitubes device for different intertube distances and the rotational angles. The solid curves labeled by the solid circles and triangles correspond to L_{t-t}=2.3 Å and 3.0 Å with the rotational angle $\varphi=0$, respectively; the dashed curves labeled by the solid circles and triangles correspond to L_{t-t}=2.3 Å and 3.0 Å with the rotational angle $\varphi=2\pi/16$, respectively; and the solid curve labeled by the asterisk corresponds to L_{t-t}=3.0 Å, L_{e-t}=2.3 Å, and $\varphi=2\pi/16$. The inset gives a comparison of the $I-V$ curves between the monotube device and the bitubes device with L_{t-t} =3.0 Å and the rotational angle $\varphi=2\pi/16$.

MPSH contains the molecule-lead coupling effects.[33,34] In fact, the density distributions of the orbit can reflect the electrode-tube coupling and intertube interaction in picturesque way. Figures 3(a1)–(a6) show six frontier molecular orbits of the MPSH for the monotube system: Orbits 254–259 correspond to HOMO−1, highest occupied molecular orbital (HOMO), lowest unoccupied molecular orbital (LUMO), LUMO+1, LUMO+2, and LUMO+3, respectively. Figures 3(b1)–(b6) and (c1)–(c6) show six frontier molecular orbits from HOMO−1 to LUMO+3 for the bitubes system with intertube distance L_{t-t}=3.0 Å and L_{t-t} =2.3 Å, respectively. It is known that a delocalized molecular orbital means the transmission channel being opened, thus yields a peak in the transmission spectra. In general, a delocalized molecular orbital contributes more to the transmission probabilities than a localized one in molecular device. From Fig. 3, it is seen that when intertube distance takes L_{t-t}=2.3 Å, almost all explored frontier molecular orbitals are delocalized, which indicates these conductance channels are opened. This shows that the shorter the intertube distance, the stronger the intertube interaction, and the more transport channels can be opened. The collective effects among molecular orbitals are responsible for the bigger transmission coefficients presented in Fig. 2(b). It should be noted in particular that it is difficult to establishing a correspondence between the transmission peaks or valleys and molecular orbitals due to the fact that in such a large molecular system the molecular orbitals are very close to each other in energy and difficult to determine which one contributed to the certain transmission peak or valley.

Figure 4 shows the current-voltage characteristics for different intertube distances and rotational angle. The electronic structure is determined self-consistently for each bias. The current is calculated by means of the Landauer–Buttiker formula:[35] $I=\int_{\mu_L}^{\mu_R} T(E, V_b)dE$, where $T(E, V_b)$ is the transmission probability for electrons incident at an energy E through a device under a bias V_b, and μ_L and μ_R denote the electrochemical potential of the left and right leads, respectively. Since the structure is symmetric, the *I-V* curves are also symmetric with respect to the bias polarity. From the figure, some main features can be addressed as follows: (i) From the current-voltage curve of the bitubes systems with short intertube distance L_{t-t}=2.3 Å, we can see clearly the linear characteristic, which indicates the system being of the metallic behavior obviously. With the increase in intertube distance, electrode-tube distance, or the rotational angle, the current is decreased remarkably. (ii) For the systems with long electrode-tube distance L_{e-t}=2.3 Å and larger rotational angle $\varphi=2\pi/16$, the *I-V* curve is flattened over a small bias range, where the current approaches zero. This is indicative of a semiconducting-like characteristics of the system. From the inset of Fig. 3, it can be found that for the same bias, the current of bitubes system is larger than twice that of the monotube system, even for the system with the rotational angle $\varphi=2\pi/16$, which indicates that the intertube interaction can enhance the electron transport evidently. These phenomena can be understood. From infinite bitubes system,[28] it is known the intertube interaction can induce the orbit splitting. And the magnitude of the splitting is dependent on the intertube distance and the rotational angle. These additional orbits offer electron transport channels and contribute to the current, which results to the increase of the total current of the bitube systems.

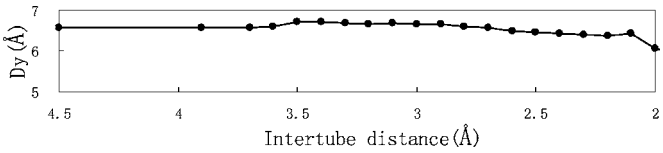

FIG. 5. Dependence of the diameter of tube on the intertube distances.

One may inquire if there exists a deformation of the tubes caused by the intertube interaction. We will indicate by calculations that the intertube interaction does not give rise to deformation of the tubes for the explored range of the intertube distance. In Fig. 5, by performing a first-principle simulations of intertube interaction, we give the dependence of the diameter of tubes on the intertube distances. The results show that when intertube distance is larger than 2.3 Å, the diameter of tube seems to be insensitive to the intertube distance. About L_{t-t}=2.3 Å, the intertube interaction causes only a very small radial deformation of the tubes.

IV. SUMMARY

In conclusion, using first-principle quantum transport calculations, we have investigated the transmission properties of electrons in a bitube device. The intertube interaction has been analyzed in detail. The results show some interesting physical effects. The intertube interaction can induce the orbit splitting, which is dependent on the intertube distance

and the rotational angle. These additional orbits offer electron transport channels and contribute to the current. By adjusting the intertube distance and the rotational angle (namely changing the magnitude of the intertube interactions), a different transport behavior can be found in the system. These results may also be helpful in understanding the transmission mechanism of other kinds of bimolecule or multimolecule systems.

ACKNOWLEDGMENTS

This work was supported by the National Natural Science Foundation of China (Grant Nos. 90403026 and 10674044) and by Hunan Provincial Natural Science Foundation of China (Grant No. 06JJ20004).

[1]M. A. Reed, C. Zhou, C. J. Muller, T. P. Burgin, and J. M. Tour, Science **278**, 252 (1997).
[2]S. N. Yaliraki and M. A. Ratner, J. Chem. Phys. **109**, 5036 (1998).
[3]S. N. Yaliraki, A. E. Roitberg, C. Gonzalez, V. Mujica, and M. A. Ratner, J. Chem. Phys. **111**, 6997 (1999).
[4]M. Di Ventra, S. T. Pantelides, and N. D. Lang, Appl. Phys. Lett. **76**, 3448 (2000).
[5]J. Reichert, R. Ochs, D. Beckmann, H. B. Weber, M. Mayor, and H. v. Lohneysen, Phys. Rev. Lett. **88**, 176804 (2002).
[6]Y. Luo and Y. Fu, J. Chem. Phys. **117**, 10283 (2002).
[7]B. Xu and N. J. Tao, Science **301**, 1221 (2003).
[8]C.-K. Wang and Y. Luo, J. Chem. Phys. **119**, 4923 (2003).
[9]K. Stokbro, J. Taylor, and M. Brandbyge, J. Am. Chem. Soc. **125**, 3674 (2003).
[10]S.-H. Ke, H. U. Baranger, and W. Yang, J. Am. Chem. Soc. **126**, 15897 (2004).
[11]P. Tarakeshwar, J. J. Palacios, and D. M. Kim, J. Phys. Chem. B **110**, 7456 (2006).
[12]W. Hu, H. Nakashima, K. Furukawa, Y. Kashimura, K. Ajito, and K. Torimitsu, Appl. Phys. Lett. **85**, 115 (2004).
[13]W. Hu *et al.*, Phys. Rev. Lett. **96**, 027801 (2006).
[14]H. Park, J. Park, A. K. L. Lim, E. H. Anderson, A. P. Alivisatos, and P. L. McEuen, Nature (London) **407**, 57 (2000).
[15]J. Taylor, H. Guo, and J. Wang, Phys. Rev. B **63**, 121104 (2001).
[16]S. J. Tans, A. R. M. Verschueren, and C. Dekker, Nature (London) **393**, 49 (1999); Z. Yao, H. W. C. Postma, L. Balents, and C. Dekker, *ibid.* **402**, 273 (1999).
[17]S. Iijima, Nature (London) **354**, 56 (1991).
[18]S. Frank, P. Poncharal, Z. L. Wang, and W. A. de Heer, Science **280**, 1744 (1998).
[19]R. Saito, G. Dresselhaus, and M. S. Dresselhaus, *Physical Properties of Carbon Nanotubes* (Imperial College Press, London, 1998).
[20]P. Pomorski, C. Roland, and H. Guo, Phys. Rev. B **70**, 115408 (2004).
[21]Y. Xue and M. A. Ratner, Phys. Rev. B **70**, 205416 (2004).
[22]J. Wu, J. Zang, B. Larade, H. Guo, X. G. Gong, and F. Liu, Phys. Rev. B **69**, 153406 (2004).
[23]Q. Yan, J. Wu, G. Zhou, W. Duan, and B.-L. Gu, Phys. Rev. B **72**, 155425 (2005).
[24]J. Cumings and A. Zettl, Science **289**, 602 (2000); Phys. Rev. Lett. **93**, 086801 (2004).
[25]B. Bourlon, C. Miko, L. Forro, D. C. Glattli, and A. Bachtold, Phys. Rev. Lett. **93**, 176806 (2004).
[26]A. A. Maarouf, C. L. Kane, and E. J. Mele, Phys. Rev. B **61**, 11156 (2000).
[27]M. J. O'Connell, S. Sivaram, and S. K. Doorn, Phys. Rev. B **69**, 235415 (2004).
[28]X. Yang, L. Chen, Z. Shuai, Y. Liu, and D. Zhu, Adv. Funct. Mater. **14**, 289 (2004).
[29]F. Wang *et al.*, Phys. Rev. Lett. **96**, 167401 (2006).
[30]J. Taylor, H. Guo, and J. Wang, Phys. Rev. B **63**, 121104(R) (2001); **63**, 245407 (2001).
[31]M. Brandbyge, J. L. Mozos, P. Ordejon, J. Taylor, and K. Stokbro, Phys. Rev. B **65**, 165401 (2002).
[32]Y. Wei, J. Wang, H. Guo, and C. Roland, Phys. Rev. B **64**, 115321 (2001).
[33]K. Stokbro, J. Taylor, M. Brandbyge, J. L. Mozos, and P. Ordejon, Comput. Mater. Sci. **27**, 151 (2003).
[34]H. Geng, S. Yin, K.-Q. Chen, and Z. Shuai, J. Phys. Chem. B **109**, 12304 (2005).
[35]M. Buttiker, Y. Imry, R. Landauer, and S. Pinhas, Phys. Rev. B **31**, 6207 (1985); M. Buttiker, Phys. Rev. Lett. **57**, 1761 (1986); IBM J. Res. Dev. **32**, 317 (1988); Phys. Rev. B **38**, 9375 (1988).